



Supporting Online Material for

Protein Synthesis and Neurotrophin-Dependent Structural Plasticity of Single Dendritic Spines

Jun-ichi Tanaka, Yoshihiro Horiike, Masanori Matsuzaki, Takashi Miyazaki, Graham C. R. Ellis-Davies, Haruo Kasai*

*To whom correspondence should be addressed. E-mail: hkasai@m.u-tokyo.ac.jp

Published 28 February 2008 on *Science Express*

DOI: 10.1126/science.1152864

This PDF file includes:

Materials and Methods
SOM Text
Figs. S1 to S7
References

Correction: The names of companies that supplied several different compounds used by the authors were added.

Protein-Synthesis and Neurotrophin Dependent Structural Plasticity of Single Dendritic Spines

Jun-ichi Tanaka, Yoshihiro Horiike, Masanori Matsuzaki, Takashi Miyazaki,
Graham C. R. Ellis-Davies & Haruo Kasai

Supporting Online Material

Materials and Methods

Preparation of slice cultures

Hippocampal slices with a thickness of 350 μm were prepared from 6- to 8-day-old Sprague-Dawley rats. Slices were mounted on 0.4- μm culture inserts and incubated at 35°C under 5% CO_2 in medium comprising 50% MEM, 25% Hanks' balanced salt solution, 25% horse serum, and glucose (6.5 g/l). After culture for 8 to 12 days, slices were transferred individually to a recording chamber and superfused at room temperature (23° to 25°C) with a solution (ACSF) that contained 125 mM NaCl, 2.5 mM KCl, 3 mM CaCl_2 , 1 mM MgCl_2 , 1.25 mM NaH_2PO_4 , 26 mM NaHCO_3 , and 20 mM glucose and which was bubbled with 95% O_2 and 5% CO_2 . For synaptic stimulation without spikes (in the absence or presence of BDNF), MgCl_2 was omitted from the solution and tetrodotoxin (1 μM) was added. The bathing solution also contained 200 μM Trolox.

In experiments with AP5 (50 to 100 μM) or K252a (200 nM), slices were superfused for at least 20 min with inhibitor before uncaging of MNI-glutamate. Slices were either preincubated with 25 μM anisomycin for 60 min or both preincubated with 5 μM anisomycin for 60 min and subjected to whole-cell perfusion with 5 μM anisomycin. Slices were incubated with cycloheximide (300 μM) for 60 min before uncaging. They were exposed to the antibody to TrkB (clone 47; BD Transduction Laboratories, Lexington, KY) at a concentration of 1 $\mu\text{g}/\text{ml}$ for 1.5 to 2 h or to TrkB-Fc (2 $\mu\text{g}/\text{ml}$; R&D Systems, Minneapolis, MN) for at least 10 min before uncaging. For experiments with TrkB-Fc and BDNF (20 ng/ml; PeproTech, Rocky Hill, NJ), bovine serum albumin (1 $\mu\text{g}/\text{ml}$) was also added to the bathing solution to prevent the loss of these proteins by nonspecific binding to the siliconized tubing and slice chamber. The experimental protocol was approved by the animal experimental committee of the Faculty of Medicine, University of Tokyo.

Two-photon excitation imaging and uncaging

Time-lapse two-photon imaging of dendritic spines was performed with an upright microscope equipped with a water-immersion objective lens (LUMPlanFI/IR 60 \times , numerical aperture of 0.9) and with Fluoview software (Olympus). Two mode-locked femtosecond-pulse Ti:sapphire lasers set at wavelengths of 720 nm (for uncaging) and 830 nm (for imaging) were connected to the laser-scanning microscope via two independent scanheads. Second or third dendritic branches were used for imaging and uncaging experiments. Three-dimensional reconstructions of dendritic morphology were generated by the summation of fluorescent values at each pixel in 17 to 23 xy-images each separated by 0.5 μm . The fluorescence of dendrites continued to

increase gradually even 20 min after whole-cell perfusion and was corrected by the entire fluorescence of a dendritic region. Volume of spine heads was estimated as described previously (S1, S2). Spine length was determined as the distance between the outlines of the parent dendritic shaft and the spine head. The peak fluorescence intensity of spine necks was measured from the fluorescence profiles of the neck at the narrowest position after correction by the background intensity near the spine before uncaging.

Precise uncaging was ensured by imaging the region of interest with the uncaging galvanometer immediately before irradiation. MNI-glutamate (4-methoxy-7-nitroindolyl-glutamate) (12 mM) was then applied locally from a glass pipette positioned close to the selected dendrite. Repetitive (1 Hz, 80 times) photolysis of MNI-glutamate was performed at 720 nm with a pulse-train duration of 0.6 ms. The amount of photoreleased glutamate was adjusted by changing the laser power (~6 mW) so as to evoke currents through α -amino-3-hydroxy-5-methylisoxazole-4-propionic acid (AMPA)-sensitive glutamate receptors with an amplitude (~5 to 20 pA) similar to that of miniature excitatory postsynaptic currents (S3).

Individual spines were stimulated by two-photon uncaging of MNI-glutamate (S3) at a wavelength of 720 nm. For pairing of synaptic stimulation with postsynaptic spikes (uncaging plus spikes), uncaging of MNI-glutamate was induced at a frequency of 1 Hz for 80 s and each train of laser pulses was followed after 10 to 15 ms by application of a single postsynaptic spike. The cells were voltage-clamped at -70 mV except during uncaging plus spikes, and superfused with a solution containing 1 mM Mg^{2+} except during uncaging without spikes. For intensive synaptic stimulation in the absence of postsynaptic spikes (uncaging without spikes), we induced uncaging of MNI-glutamate at 1 Hz for 40 s in a Mg^{2+} -free solution, unless otherwise stated.

Electrophysiology

For whole-cell recordings, the patch-clamp electrode (open-tip resistance, 4 to 7 M Ω) was filled with a solution containing 120 mM potassium gluconate, 20 mM KCl, 10 mM disodium phosphocreatine, 50 μ M Alexa594 (Invitrogen), 4 mM ATP (magnesium salt), 0.3 mM GTP (sodium salt), 10 mM Hepes-KOH (pH 7.3), and 5 μ M β -actin (human platelet; Cytoskeleton, Denver, CO)(Supporting text). Series resistance was 16.6 ± 5.6 M Ω (mean \pm s.d.) and the resting membrane potential was -58.5 ± 2.9 mV (mean \pm s.d.). Cells with a resting potential of >-55 mV at uncaging were excluded from data analysis. A small hyperpolarizing holding current (10 to 50 pA) was applied when cells showed spike activities. Action potentials were elicited by injection of a depolarizing current of 1 to 2 nA for 2 ms. AMPA receptor-mediated currents were obtained by voltage-clamping cells at -70 mV when two-photon uncaging was effected at the tip of spines with a laser power of 6 mW (fig. S2). The currents were evoked three to five times at each time point, low-pass filtered at 2 kHz, sampled at 10 kHz, and averaged.

Data analysis

Two-photon images and electrophysiological data were analyzed with IPLab and Igor Pro 4 software, respectively. Statistical analysis was performed with Prism. Data are presented by means \pm s.e.m. (n = number of spines) and were analyzed by the Mann-Whitney U test unless stated otherwise. A P value of <0.05 was considered statistically significant.

Supporting Text

We found that the washout of plasticity (*S4*) was prevented by up to 20 min in the presence of β -actin (5 μ M) in the pipette (fig. S1). Enlargement was also induced in the presence of 5 μ M of α -actin prepared (by Dr. Y. Ishikawa) from skeletal muscles ($n = 4$). Thus, the washout of STDP reported in previous studies (*S4*) may arise from the time-dependent loss of β -actin during intracellular dialysis. The maintenance of STDP by addition of intracellular β -actin supports the idea that actin has a role in synaptic plasticity (*S5-S8*). The effect of β -actin on enlargement was not significant at 1 μ M ($n = 3$)(fig. S1), consistent with the fact that a high concentration of actin is necessary for the spine enlargement (*S9*). We could not examine concentrations of β -actin greater than 5 μ M, because such solutions impaired formation of giga-seals with the neuron membrane and prevented whole-cell patch clamp recording. β -actin, however, did not prevent washout of enlargement at times longer than 40 min after whole-cell perfusion ($n = 3$). The remaining washout phenomena may be explained by the presence of many actin regulator proteins in spines (*S8*). We therefore applied induction protocols about 20 min after whole-cell perfusion, when stable imaging of individual spines became possible.

Heat-inactivated BDNF (HI-BDNF) was not effective in the enhancement of the spine enlargement induced with uncaging without spikes (fig. S6A). In addition, the spine enlargement was blocked by AP5 even in the presence of BDNF (fig. S6A). Large spines did not show significant enlargement and LTP by uncaging plus spikes even in the presence of BDNF (fig. S6B), as in its absence (fig. S3, C and D).

Our results indicate that synaptic stimulation paired with postsynaptic spikes can trigger protein synthesis-independent immediate enlargement of dendritic spines, in addition to protein-synthesis dependent gradual enlargement. Each spine thus senses the temporal synchrony of spike activities between pre- and postsynaptic neurons, and immediately responds to it with enlargement. Given that a single pyramidal neuron possesses thousands of spines, each innervated by a different presynaptic neuron, the motility of numerous spines in a neuron physically encodes correlated activities of thousands of neurons in the brain. Correlated neuronal activity has been implicated in both memory acquisition and cognitive processes (*S10, S11*). Further elucidation of the dynamics of spine structure should therefore help to clarify the cellular basis of higher-order brain functions and mental disorders.

Supporting Figures

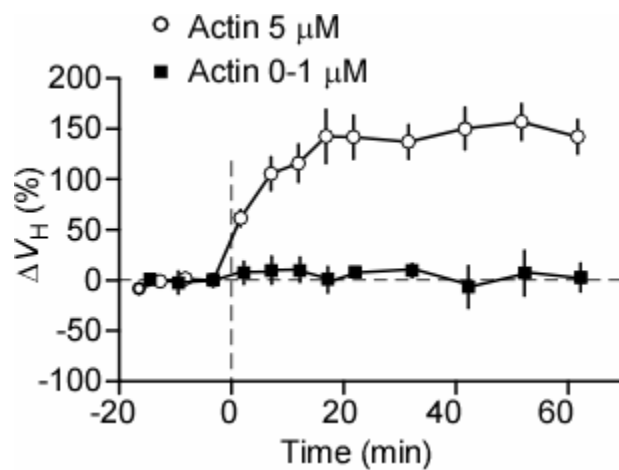


Fig. S1. Washout of spine enlargement induced with uncaging plus spikes in the cells whole-cell dialyzed with a solution containing 0 μM ($n = 5$) or 1 μM ($n = 3$) of β -actin (filled circles) for 20 min, and its prevention with a solution containing 5 μM ($n = 37$, open circles).

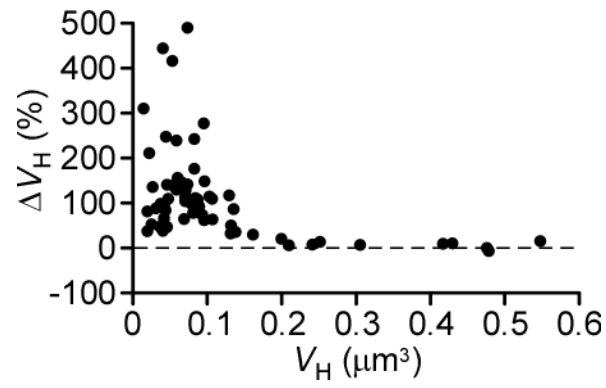


Fig. S2. Dependence of spine-head enlargement (ΔV_H) induced by glutamate uncaging paired with postsynaptic spikes on the initial spine-head volume (V_H). Spine enlargement was measured 40 to 60 min after the onset of stimulation.

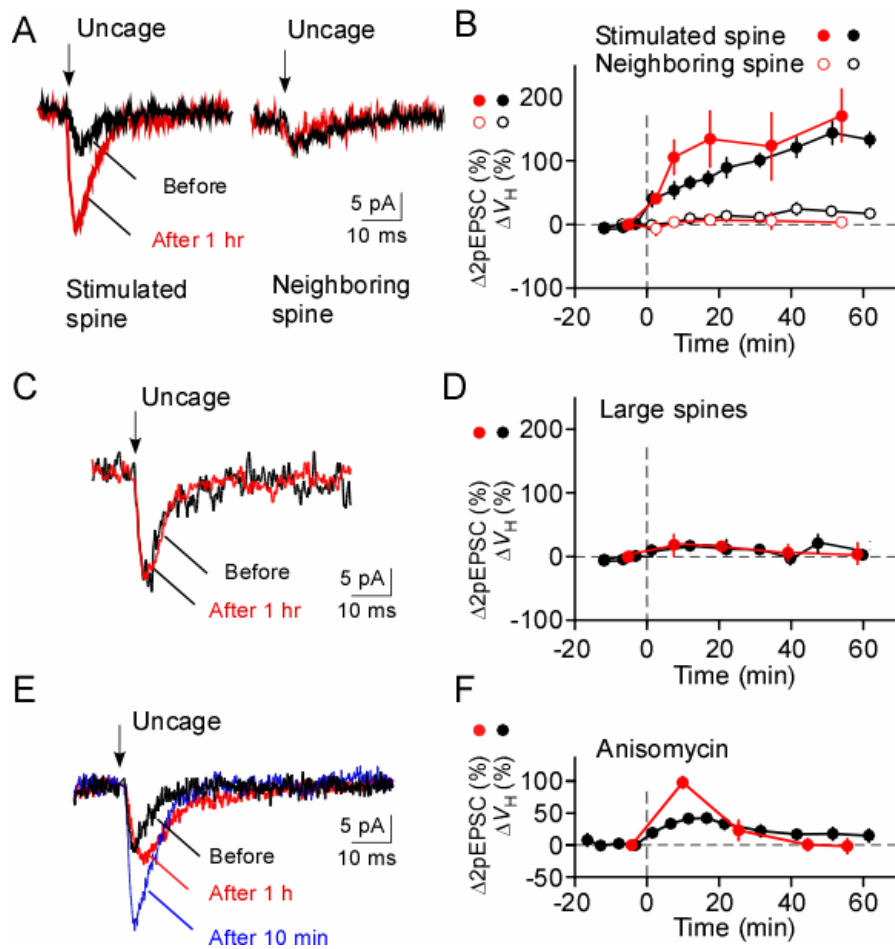


Fig. S3. Potentiation of glutamate-induced currents by glutamate uncaging paired with postsynaptic spikes. **(A)** Averaged glutamate-induced currents (in the presence of Mg^{2+}) recorded before (black) and 1 h after (red) exposure of a small spine to uncaging plus spikes. Traces are shown for both the spine exposed to uncaging plus spikes and a neighboring spine. **(B)** Mean time courses of changes in spine-head volume (ΔV_H , black) and in the amplitude of glutamate-induced currents ($\Delta 2pEPSC$, red) in small spines subjected to uncaging plus spikes (filled symbols) at time 0 and in neighboring spines (open symbols). Data are means \pm s.e.m. ($n = 12$). Initial amplitudes of 2pEPSCs were $5.4 \text{ pA} \pm 1.2 \text{ pA}$ and $5.2 \pm 1.5 \text{ pA}$ for stimulated and neighboring spines. **(C)** Averaged glutamate-induced currents recorded before (black) and 1 h after (red) exposure of a large spine with a volume of ($0.24 \mu\text{m}^3$) to uncaging plus spikes. **(D)** Mean time courses of changes in spine-head volume (ΔV_H , black) and in the amplitude of glutamate-induced currents ($\Delta 2pEPSC$, red) in large spines ($> 0.2 \mu\text{m}^3$) subjected to uncaging plus spikes (filled symbols) at time 0 ($n = 6$). **(E)** Averaged glutamate-induced currents recorded before (black), 10 min after (blue), and 60 min after (red) exposure of a small spine to uncaging plus spikes in the presence of anisomycin. **(F)** Mean time courses of changes in spine-head volume (black) and in the amplitude of glutamate-induced currents (red) in small spines subjected to uncaging plus spikes at time 0 in the presence of anisomycin. Data are means \pm s.e.m. ($n = 7$).

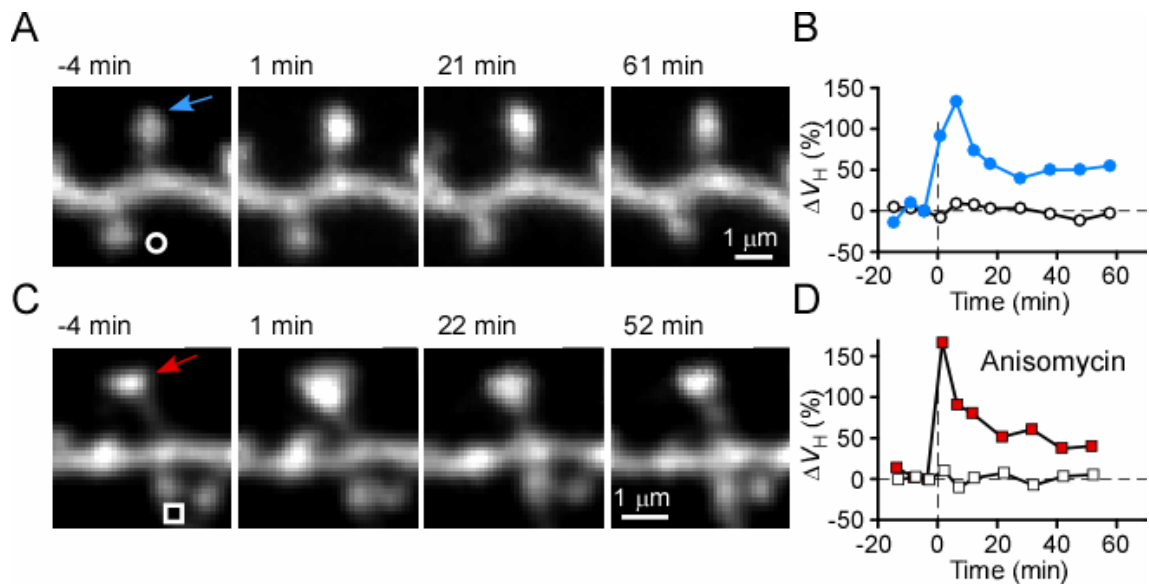


Fig. S4. Spine enlargement induced by uncaging of glutamate without spikes (in Mg^{2+} -free solution). (**A** and **C**) Time-lapse z-stack images of spines stimulated at time 0 by uncaging without spikes in the absence (**A**) or presence (**C**) of anisomycin. Arrows indicates spots of two-photon uncaging of MNI-glutamate. Open symbols indicate neighboring spines. (**B** and **D**) Time courses of changes in spine-head volume for the stimulated (filled symbols) and neighboring (open symbols) spines shown in (**A**) and (**C**), respectively.

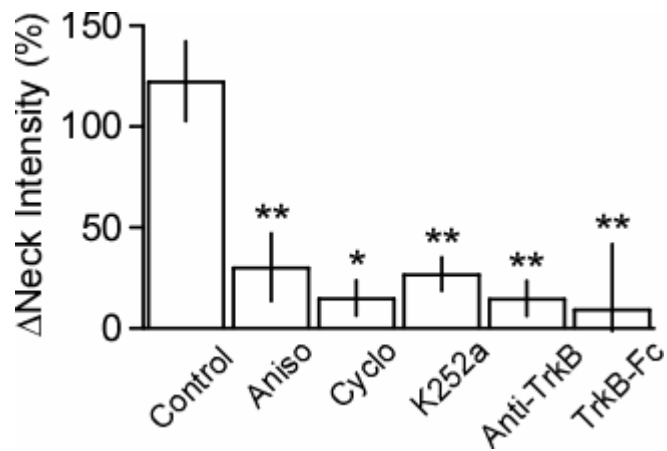


Fig. S5. Effects of inhibitors of protein synthesis or BDNF-TrkB signaling on the increase in spine-neck fluorescence intensity induced by glutamate uncaging paired with postsynaptic spikes. Stimulation was performed in the absence (control, $n = 20$) or presence of anisomycin ($n = 11$), cycloheximide ($n = 8$), K252a ($n = 13$), anti-TrkB ($n = 9$), or TrkB-Fc ($n = 10$). Data are means \pm s.e.m. * $P < 0.05$, ** $P < 0.01$ versus control value (Mann-Whitney U test).

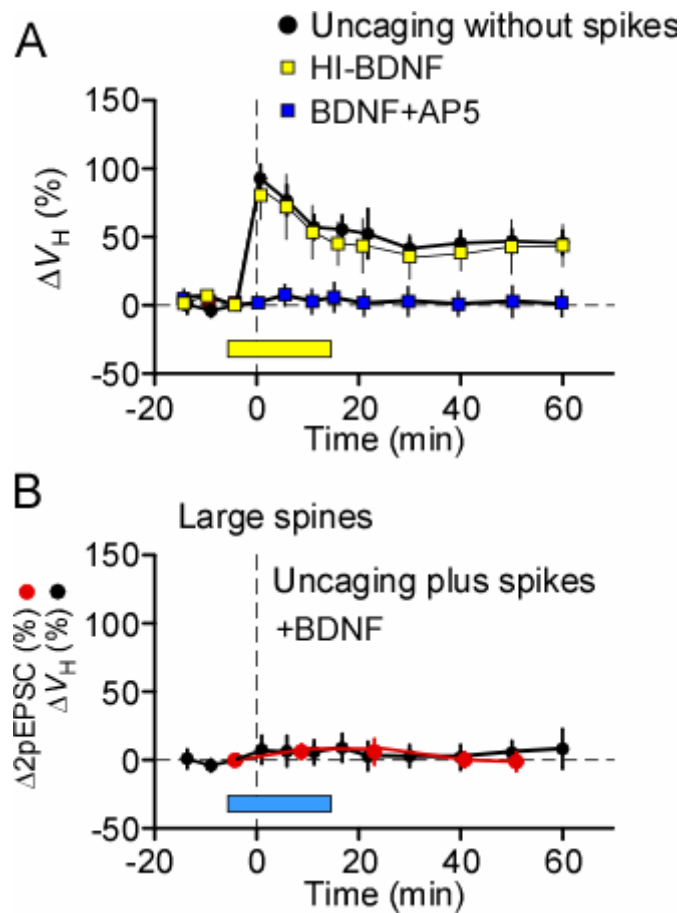


Fig. S6. (A) Effects of heat-inactivated BDNF (HI-BDNF, 95°C for 15 min)(yellow squares)($n = 7$) or BDNF (20 ng/ml) plus AP5 (20 μ M) (blue squares) ($n = 5$) on the time courses of enlargements of spines induced with uncaging with spikes in the absence of Mg^{2+} . Filled circles represent the control experiments ($n = 20$). (B) Time courses of spine volumes (black circles) and 2pEPSC (red circles) in large spines with volume $> 0.2 \mu m^3$ ($n = 6$) applied with uncaging plus spikes in the presence of BDNF.

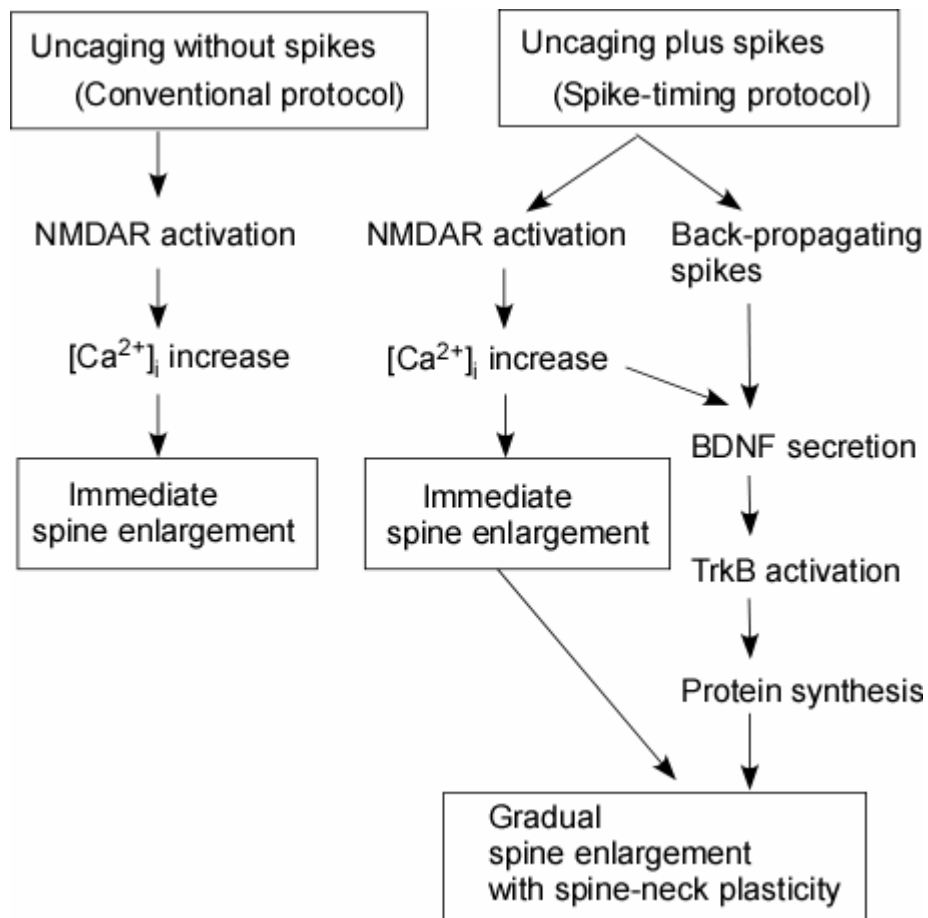


Fig. S7. Hypothetical signaling cascades for spine enlargement induced either with a conventional protocol (uncaging without spikes) or with a spike-timing protocol (uncaging plus spikes).

References

- S1. M. Matsuzaki, N. Honkura, G. C. Ellis-Davies, H. Kasai, *Nature* **429**, 761 (2004).
- S2. J. Noguchi, M. Matsuzaki, G. C. R. Ellis-Davies, H. Kasai, *Neuron* **46**, 609 (2005).
- S3. M. Matsuzaki *et al.*, *Nat. Neurosci.* **4**, 1086 (2001).
- S4. K. Kato, D. B. Clifford, C. F. Zorumski, *Neuroscience* **53**, 39 (1993).
- S5. C. H. Kim, J. E. Lisman, *J. Neurosci.* **19**, 4314 (1999).
- S6. T. Krucker, G. R. Siggins, S. Halpain, *Proc. Natl. Acad. Sci. U. S. A* **97**, 6856 (2000).
- S7. K. Okamoto, T. Nagai, A. Miyawaki, Y. Hayashi, *Nat. Neurosci.* **7**, 1104 (2004).
- S8. M. Sheng, M. J. Kim, *Science* **298**, 776 (2002).
- S9. N. Honkura, M. Matsuzaki, J. Noguchi, G.C.R. Ellis-Davies, H. Kasai, *Neuron*, in press (2008).
- S10. W. Singer, C. M. Gray, *Annu. Rev. Neurosci.* **18**, 555 (1995).
- S11. von der Malsburg, C. *Neuron* **24**, 95 (1999).